An Engineered Human Fibroblast Growth Factor-1 Derivative, TTHX1114, Ameliorates Short-term Corneal Nitrogen Mustard Injury in Rabbit Organ Cultures

David D. Eveleth,[1] Jennifer J. Eveleth,[1] Amuthakannan Subramaniam,[1] Rita Hahn,[2] Peihong Zhou,[2] Marion K. Gordon,[2] and Ralph A. Bradshaw[1]

[1]Trefoil Therapeutics, Inc., San Diego, California, United States
[2]Department of Pharmacology and Toxicology, Ernest Mario School of Pharmacy, Rutgers University, Piscataway, New Jersey, United States

PURPOSE. Organ cultures of rabbit corneas have been used to ascertain the effectiveness of a human fibroblast growth factor (FGF)-1 derivative (TTHX1114), lacking cysteine residues, to protect against and/or repair epithelial lesions following exposure to nitrogen mustard (NM).

METHODS. Rabbit corneas were exposed to NM and cultured for up to 14 days, with or without drug (TTHX1114). At specified times, tissue was examined by histopathology and graded by a novel composite scale. Proliferation was measured by 5-ethynyl-2′-deoxyuridine (EdU) incorporation, and the expression of native FGF-1 and ADAM-17 after NM exposure was determined by immunofluorescence.

RESULTS. Rabbit corneas, exposed to a single dose of NM, showed a nearly complete loss of epithelial cells by day 6 but were significantly regenerated by day 14. When treated continuously with TTHX1114 following vesicant exposure, the losses remained at day 2 levels. The loss of keratocytes in the stroma was not affected by TTHX1114. EdU incorporation over the same time course showed a steady increase in tissue that had not been treated with TTHX1114, while corneas that were treated with the drug showed a higher percent incorporation initially, which then decreased, indicating the strong proliferative response to TTHX1114. ADAM-17 was not significantly altered by TTHX1114 treatment. Corneal epithelial FGF-1 disappeared after only 1 day following exposure to NM.

CONCLUSIONS. TTHX1114 is protective against NM-induced damage of the corneal epithelium, possibly by supplying an NM-resistant source of trophic support and by stimulating regeneration of new epithelial cells. These responses underscore the potential value of TTHX1114 as an anti-vesicant therapeutic.

Keywords: epithelial cell regeneration, fibroblast growth factor-1, cell proliferation, nitrogen mustard, FGF-1 expression, ADAM-17, keratocytes

Of the three main organ targets—skin, lung, and eye—of the vesicating agents used in biological warfare, such as the nitrogen and sulfur mustards (NM and SM), the eye is perhaps the most important because of the immediate (acute) ramifications of the insult and the potential for long-term (chronic) visual impairment.[1] Exposure to these agents causes relatively rapid microvesication with deepithelialization of the corneal surface[2] that results in significant pain and degradation of vision. Increasing evidence indicates stromal and endothelial cell damage also occurs at the time of the original insult, and the extent of the injuries to these more posterior layers may be related to the onset of the chronic disease that is seen in more severely affected casualties.[3] Steroids, such as dexamethasone, have had limited use in treating the acute phase damage to the epithelial layer after mustard exposure,[4] which will generally heal itself in a few weeks with no intervention,[5,6] and organ transplants remain the only effective treatment for the chronic phase of the disease, generally known as mustard gas keratopathy (MGK).[7,8] SM is clearly more toxic than NM, and the knowledge base of vesicant effects is mainly derived from

its study; however, NM, which is more amenable to laboratory manipulations, shows sufficiently similar responses by epithelial cells to be a useful paradigm for testing potential protective agents against vesicant damage.

Although the precise mechanisms that result in cell- or tissue-specific cytotoxicities following mustard gas exposure are unknown, it is appreciated that the mustards are effective alkylating agents and appear to act in large part by derivatizing biological macromolecules, particularly nucleic acids and proteins.[9] These moieties differ in potency and effect; for example, SM is bifunctional and can cause chemical cross-linking as part of its reaction profile, while NM is only monovalent, and accordingly they do not necessarily share the same cellular targets. In proteins, cysteine has been shown to be the most reactive to NM,[10] which is consistent with the fact that the thiol group of cysteine is known to be the most reactive nucleophile in this family of macromolecules. Because these residues are in polypeptides primarily found in intracellular locations, as are the nucleic acids, it is generally assumed that the greatest toxicity is associated with modifications by

vesicant acting intracellularly. Proteins that are normally exported through the endoplasmic reticulum/Golgi continuum to function in the extracellular space undergo a net oxidation in which their cysteine residues are converted to cystine to produce both intra- and interchain disulfide bonds,[11] and these would not be expected to be significantly sensitive to alkylating agents. Exported proteins include most hormones and growth factors that interact with their target cells through cell surface receptors and regulate such processes as differentiation, proliferation, and maintenance of cell viability.

There are, however, a small number of regulatory proteins that are exported via a non-ER/Golgi pathway, and these moieties retain their cysteine residues in a reduced state[12] after leaving the intracellular environment. As such they are potential targets of SM and NM modification and inactivation. Two important members of this select group are fibroblast growth factors-1 and -2 (FGF-1 and -2), which play a key role in development among a wide variety of cellular targets,[13] including the cornea,[14,15] with upregulation of FGF and FGF receptors in the epithelium[16-18] and acceleration of ocular surface wound healing in animals and humans by exogenously added FGFs.[19,20] These two members of the much more extensive FGF family each contain three cysteine residues and are inactivated by their oxidation.[21] Thus exposure to mustard gas would lead to their inactivation without requiring intracellular invasion of the vesicant. Derivatives of FGF-1 that lack cysteine have been made, and these molecules are more potent than unmodified FGF-1 in stimulating mitogenesis and are more stable in biological systems.[21,22] One such derivative, TTHX1114, has been modified to eliminate all reactive cysteines by replacing two of the three native Cys residues with nonreactive residues and with the introduction of a new Cys residue (A66C) that forms an intrachain disulfide bond with the remaining Cys at position 83. This entity retains its natural binding site for heparin, although it can function without it.[23]

The efficacy of both endogenously produced and exogenously applied FGFs in the context of mustard gas injury may be limited by this sensitivity to cysteine modification. It is unclear to what extent the inactivation of native FGF-1 may contribute to epithelial cell loss in mustard-induced injury and whether residual vesicant would impair the ability of exogenously added drugs that were sensitive to cysteine modification. To assess the effect of native FGF-1 on vesicant injury and to determine whether an FGF-1 derivative lacking reactive thiol groups would be effective in mitigating mustard injury, a rabbit organ culture model, along with an objective histopathological grading scale, has been developed and the effectiveness of TTHX1114 in countering NM injury in the short term examined.

MATERIALS AND METHODS

Reagents

Human engineered FGF-1(TTHX1114) (C16S/A66C/C117V wherein A66C forms an intrachain disulfide bond with C83) was prepared as a 140–amino acid protein commencing with N-terminal Phe by Trefoil Therapeutics, Inc. (San Diego, CA, USA). The expression construct used contained an amino terminal extension with a poly-His sequence for purification purposes that was removed by enterokinase; the resulting 140-residue product was further purified to essential homogeneity prior to use. Mouse monoclonal anti-human FGF-1 was obtained from Abcam (ab117640 [clone: 2E12]; Cambridge, UK), and donkey anti-mouse secondary antibody was from Jackson ImmunoResearch (DyLight 549; West Grove, PA, USA).
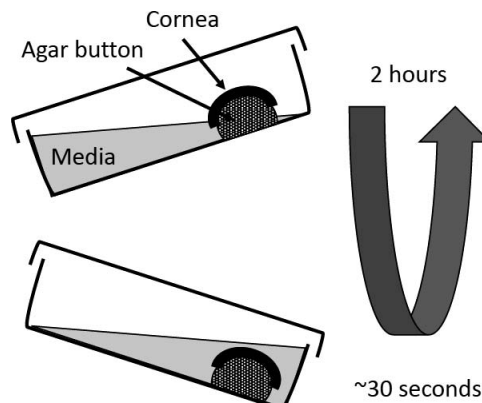

FIGURE 1. Schematic diagram of in vitro cornea rocker platform. Corneas were placed on preformed agar buttons (*green*) that have been previously secured asymmetrically to 20 × 100-mm Petri dishes with liquid agar. Fifteen milliliters of media was added to each Petri dish such that the cornea was not in contact with the media in the horizontal position. The rocker platform tilt was set so that the agar button and cornea were submerged at the apex of the 2-hour cycle (*bottom*) and were largely exposed to air at the opposite tilt angle (*upper*). The submersion phase was for 30 seconds; the remaining time of the 2-hour cycle left the corneas exposed to air. Experiments were carried out at 37°C.

Corneal Organ Culture

Whole rabbit eyes were purchased (Pel-Freez, Rogers, AR, USA) and were rinsed in povidone iodide, washed in PBS (pH 7.4; Gibco, Grand Island, NY, USA) followed by corneal excision leaving a 2-mm scleral ring around the corneal periphery. Corneas were draped over 500 μL agar buttons that were precast in a gumdrop mold (Scottcrew Enterprises, Spring Lake, MI, USA), composed of 1.5% agar in Dulbecco's modified Eagle's medium (DMEM) with 4500 mg/L glucose, L-glutamine, and sodium pyruvate (Mediatech, Manassas, VA, USA) and placed in 20 × 100-mm Petri dishes. The buttons were secured to the dish using melted agar and placed in the dishes approximately 40 mm from the center or closer to the edge of the dish. Each dish was filled with 15 mL culture media composed of DMEM as described above, supplemented with Roswell RPMI 1640 vitamin solution 100 × 10-mL/L (R7256; MilliporeSigma, St. Louis, MO, USA), MEM amino acids 10 mL/L (no. 11140; Invitrogen, Carlsbad, CA, USA), antibiotic antimycotic 10 mL/L (no. 15240-062; Invitrogen), ascorbic acid 250 mM 1 mL/L (MilliporeSigma), ascorbic acid 2-P 225 mM 2 mL/L (MilliporeSigma), and 10 mg/L ciprofloxacin (Fluka/Sigma no.17850; MilliporeSigma).[24,25] The corneas in the Petri dishes were placed on a rocker platform with the corneas in each dish oriented such that when the rocker was at the maximum tilt, the corneas were exposed to air, and when halfway through one complete cycle, they were submerged in media (Fig. 1).

NM Exposure

Corneas were processed for organ culture as above and maintained in culture for 2 days to allow recovery from the enucleation/excision process. Two days post dissection (designated as day 0 of treatment), the media was drained from the dishes and 10 μL of freshly prepared 10 mM NM (mechlorethamine) (MilliporeSigma) in culture media was applied to the center of the cornea. After 2 hours at room temperature, the corneas were rinsed three times with culture media and then placed in culture media alone or in culture

TABLE 1. Histopathological Grading Scale for Vesicant Damage

Total Epithelial Differentiation
1. Normal three layer, good differentiation
2. Disruption in layers, differentiation
3. Single layer only
4. Single layer, partial coverage
5. No epithelium present

Basal Layer (BL)
1. Columnar formation proper orientation
2. Columnar and rounded with minor orientation changes
3. Rounded, erratic orientation
4. Rounded, erratic orientation, partial coverage
5. No BL present

EIA
1. No breaks in EIA
2. Mild breaks, vesicles appear in EIA
3. Moderate breaks, vesication in EIA
4. No EIA observed
5. No epithelium present

Each corneal cross-section at the lesion site was evaluated for total epithelial differentiation, BL, and EIA. Scores for the three criteria were then summed, and mean and standard deviations generated.

media containing TTHX1114, 100 pg/mL, and returned to the incubator. Control or naive corneas were not exposed to NM but were subjected to the same room temperature rinse and media change protocol.[24,25]

Fixation and Staining of Corneas

At specified time points post NM exposure (days 2, 4, 6, 9, and 14), the corneas were harvested and fixed with 2% paraformaldehyde in PBS for 2 hours at room temperature and processed for paraffin embedment. The corneas were then cross-sectioned at a thickness of 4 μm and stained with hematoxylin and eosin (H&E) for histopathological evaluation.[26]

Corneal Histologic Grading Score

In vitro corneal epithelium health at the lesion site for each cornea was evaluated by three criteria: (1) epithelial differentiation, (2) basal layer orientation, and (3) epithelial intracellular adhesion (EIA) (Table 1; Fig. 2). Scores were assigned to each group based on a scale from 1 (no or minimal change) to 5 (loss of epithelial structures) for each criterion. The score for the three criteria was summed to give an overall rating that ranged from 3 (best) to 15 (complete loss of the epithelial layer). Thus, the lower the score, the healthier the tissue. The mean and standard deviation was calculated for each group and time point ($n = 8$).

Stromal Histologic Grading Score

In vitro corneal stromal health at the lesion site for each cornea was evaluated by two criteria: (1) stromal structure and (2) keratocytes (Table 2; see also Fig. 7). Scores were assigned using the scales described in Table 2 and the two criteria scores summed to give an overall rating that ranged from 2 (best) to 9 (worst). Mean and standard deviation were calculated for each group and time point ($n = 8$).
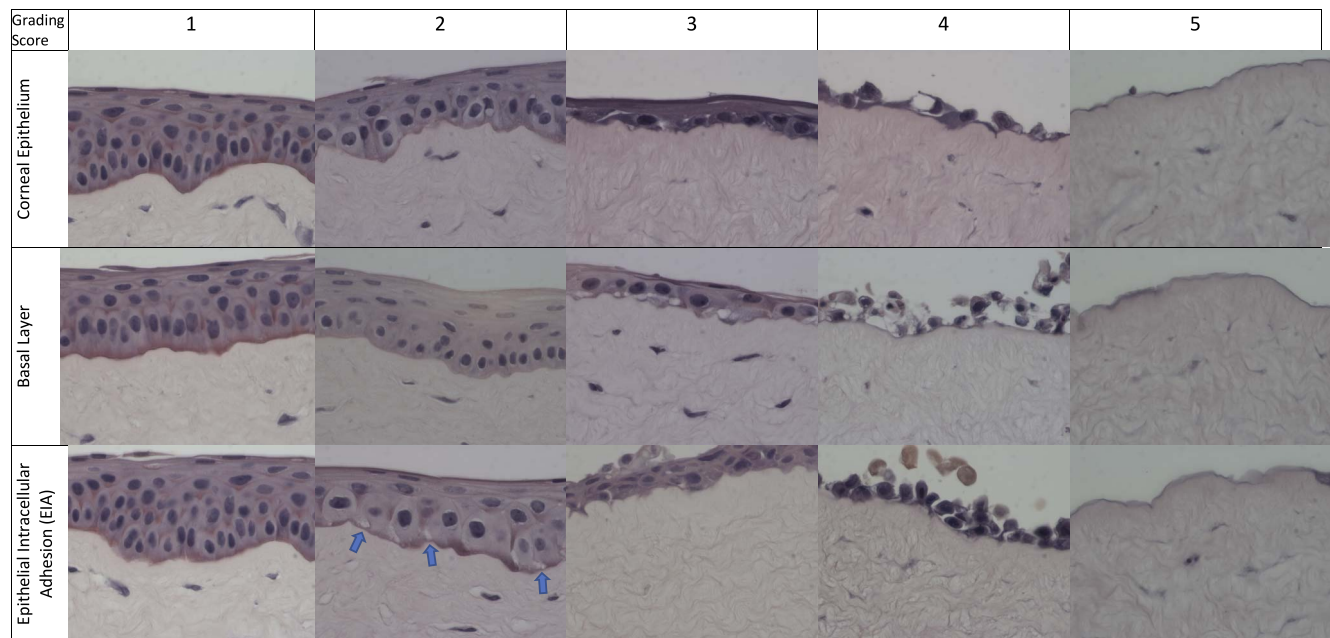

FIGURE 2. Rabbit corneal epithelial grading scale. Micrographs of in vitro rabbit epithelium in organ culture illustrating epithelial grading. *Row A* (l-r): Epithelial differentiation (graded 1–5). (**1**) Epithelium displays three layers of cellular differentiation (basal, suprabasal, superficial basal). (**2**) Clear definition between layers and differentiation mildly compromised. (**3**) Single layer of epithelium present. (**4**) Single layer of epithelium partial coverage. (**5**) No epithelium present. *Row B* (l-r): Basal epithelial layer (graded 1–5). (**1**) Columnar basal cells oriented perpendicular to the basement membrane. (**2**) Areas of basal cells begin to round, loss of orientation. (**3**) Basal cells rounded. (**4**) Basal cells with lack of continuous coverage. (**5**) No basal layer present. *Row C* (l-r): EIA (graded 1–5). (**1**) No breaks between epithelial cells seen. (**2**) Vesicles begin to form at the basal layer and between cells (*arrows*). (**3**) Further breaks appear between epithelial cells. (**4**) Severe loss of adhesion between epithelial cells. (**5**) No epithelium present. Magnification 800×.

TABLE 2. Histopathological Grading Scale for Stromal Vesicant Damage

Stromal Structure
1. No disruption noted
2. Mild separation of keratocytes from stroma
3. Moderate separation of keratocytes from stroma
4. Severe separation of keratocytes from stroma

Keratocytes
1. Present, in normal orientation to epithelial layer
2. Abnormal shape and orientation to epithelial layer mild
3. Abnormal shape and orientation to epithelial layer moderate
4. Abnormal shape and orientation to epithelial layer severe
5. No keratocytes present below epithelial layer

Each corneal cross-section at the lesion site was evaluated for the stromal structure and keratocytes; scores for the two criteria were then summed, and mean and standard deviations generated.

5-Ethynyl-2′-deoxyuridine (EdU) Labeling and Staining Corneas

Imaging kits were used for EdU labeling and staining (Click-iT EdU; Invitrogen). Following exposure to TTHX1114, the cultured corneas were treated at specified time points with EdU (5 μM) for 24 hours. After incubation, the corneas were harvested and placed in 2% paraformaldehyde in PBS, fixed for 2 hours at room temperature, and transferred to 70% ethanol for paraffin embedment. Three 4-μm cross sections of the cornea were placed on microscope slides and permeabilized (Triton X-100; MilliporeSigma). Cornea sections were stained by incubating for 30 minutes with Click-iT reaction cocktail containing Alexa Fluor 488 azide and $CuSO_4$. The staining mix was freshly prepared each time and was used within 15 minutes of preparation. The sections were counterstained with Hoechst 33342 for 30 minutes and imaged by fluorescence microscopy. The data were collected peripherally, starting just above the limbal area and proceeding to the lesion edge on both sides of the section. This peripheral counting was selected to allow comparison of the corneas between time points in varying states of lesioning against each other. Percent of EdU incorporation of epithelial basal cells peripheral to the lesion site was calculated as total EdU-labeled cells divided by the number of total basal cells.

ADAM17 Imaging

Rabbit corneas from the organ culture system were embedded in ornithine carbamoyltransferase (OCT) (TissueTek; Sakura Finetek USA, Torrance, CA, USA), frozen using a dry ice/isopentane bath, and stored at −70°C until use. Cryosections (6 μm) on slides were fixed in −20°C methanol for 10 minutes and nonspecific binding blocked by incubation with 5% normal goat serum (NGS) (MilliporeSigma) in PBS with 0.05% Tween-20 (MilliporeSigma). Sections were incubated for 1 hour in 5 μg/mL antibody to human ADAM-17 (MAB 9304; R&D Systems, Minneapolis, MN, USA) in PBS with 1.5% NGS at room temperature, washed three times with PBS with 0.05% Tween-20, and incubated for 1 hour with goat anti-mouse immunoglobulin G (IgG)–Alexa Fluor 488 conjugate (Invitrogen) 1:1000 in PBS with 1.5% NGS. After washing three times with PBS with 0.05% Tween-20, sections were coverslipped using Vectasheild hard set antifade mounting medium with 4′,6-diamidino-2-phenylindole (DAPI) (Vector Laboratories, Burlingame, CA, USA).[17,18]

FGF-1 Expression

For FGF-1 immunostaining, corneas were placed in OCT and set on an ice bath for 30 minutes, then frozen on the surface of liquid nitrogen.

OCT-embedded sections were allowed to air dry before outlining sections with a PAP pen. Sections were rehydrated with 3 × 10 minute washes of PBS/Tween-20. Sections were blocked with 5% normal donkey serum in PBS/Tween-20 for 1 hour at room temperature. Mouse monoclonal anti-human FGF-1 was diluted to 30 μg/mL in 1.5% normal donkey serum/PBS/Tween-20, applied to designated sections, and incubated at 4°C, overnight. Sections were washed again 3 × 10 minutes. Donkey anti-mouse secondary antibody diluted 1:400 in 1.5% normal donkey serum with PBS/Tween-20 was applied accordingly and incubated 1 hour at room temperature in the dark. Sections were washed 3 × 10 minutes in PBS/Tween-20. (Negative controls were sections with no primary but with secondary antibody and no primary-no secondary antibody.) Slides were washed 3 × 10 minutes and mounted with mountant and DAPI (Prolong Gold; Invitrogen-Life Technologies, Eugene, OR, USA). Digital images were captured using an inverted fluorescent microscope using a camera and imaging software (Zeiss and ProgResCaturePro; Jenoptik Optical Systems, Jena, Germany).

RESULTS

Corneal Histologic Grading Score

As a means of making a more quantitative assessment of the NM-induced damage to the corneal epithelium, a composite grading score that evaluates three distinct parameters was devised: (1) epithelial differentiation, (2) basal layer orientation, and (3) EIA. In each case, five levels of increasing severity were defined (Table 1), ranging from a normal, unlesioned epithelium (level 1) to a complete loss of the epithelia cell layer (level 5). A number (level) was assigned for each category for any given image and then summed to give the final score. An image corresponding to each level in the three different categories is shown in Figure 2. In category 1 (top row), the corneal epithelium was graded for overall differentiation and integrity. As damage progressed, there was a loss of epithelial organization and layering, progressing to partial epithelial coverage and loss of epithelial layer completely. Noteworthy is the reduction in the top and middle layers in 2, with elimination of the middle layer in 3 and no discernible layering in 4, with no cells at all in 5. In category 2 (middle row), there was a decrease in density of the basal layer and rounding of basal layer cells at level 2, a lack of columnar structure of the basal layer at level 3, rounded and erratic cells at level 4, and no cells at all at level 5. In category 3 (bottom row), EIA analysis showed there were gaps between basal layer cells at level 2, gaps in all cell layers at level 3, extensive cell separation at level 4, and no cells at all at level 5.

Effect of TTHX1114 on Corneal Epithelial Cells in Organ Culture

A 2-week time course of corneal epithelium response to NM exposure at day 0 is shown in Figure 3a (top row). By comparison to the scale illustrated in Figure 2, all components of the composite score were at or near 5, yielding final values approaching 15 by day 6. These findings are consistent with previous reports of vesicant-induced epithelial damage.[3] By day 14, natural regenerative processes had largely restored the epithelium to level 2 to 3 in all categories. The bottom row of this figure shows the same experimental time course carried
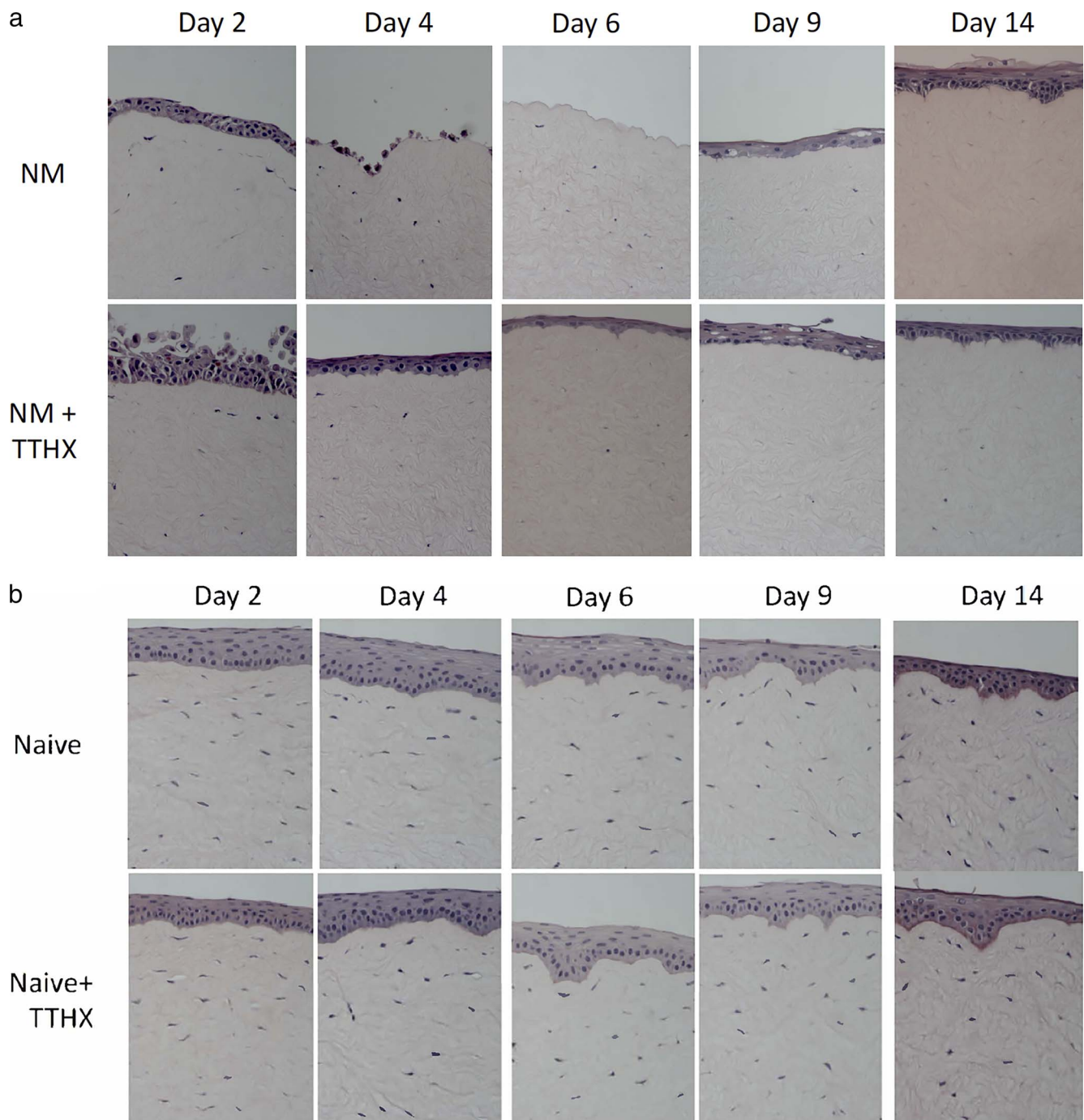
FIGURE 3. **(a)** Lesion evolution assessed by H&E. In vitro rabbit corneal micrographs stained by H&E representing tissue changes post NM-induced lesioning as a function of time with and without TTHX1114. All corneas were exposed to 10 μL 10 mM NM at day 0. TTHX1114 (100 pg/mL) was added to the culture media 2 hours post NM exposure (*row 2*). All media was changed daily. Magnification 200×. **(b)** In vitro naive (non-NM-lesioned) rabbit corneal micrographs stained by H&E taken at the same time points as in Figure 3a. TTHX1114 (100 pg/mL) was added to the culture media in the same fashion as described in Figure 2a (*row 2*). All media was changed daily. Magnification 200×.

out with 100 pg/mL of TTHX1114 in the media. In contrast to the severe losses seen at day 4 and particularly at day 6 in the NM-lesioned corneas without TTHX1114, the drug-treated corneas show significantly less damage with only level 2 to 3 lesions throughout the 2-week period. Grading of images from groups of corneas ($n = 8$ per time point per condition) using the scale shown in Table 1 shows that the NM-induced damage peaks at 6 days and that treatment with TTHX1114 post NM exposure protects the corneas from damage, with the

TTHX1114-treated corneas maintaining a lower (better) score at days 4, 6, and 9 (Fig. 4) with *P* values for the individual comparisons at these three times of 0.0014, 0.0005, and 0.0314, respectively. By comparison, the lesioned corneas not treated with drug showed this score only on days 2 and 14, being significantly higher (indicating greater damage) for the other three time points (days 4, 6, and 9).

The effect of TTHX1114 on corneas maintained under the same conditions (but not exposed to NM) is shown in Figure
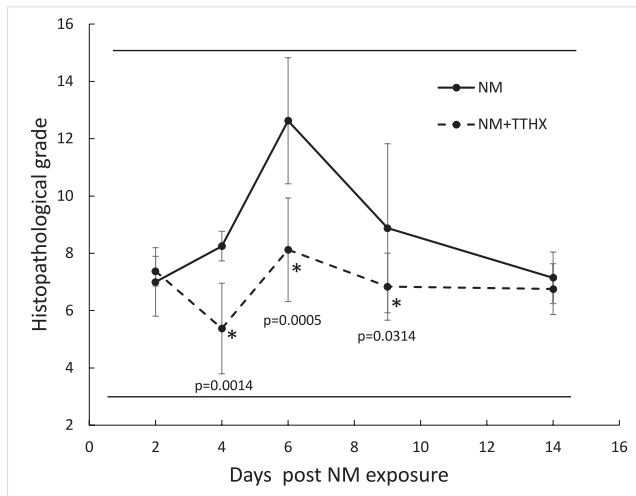
FIGURE 4. The effect of TTHX1114 on NM lesions in in vitro rabbit corneal epithelia as a function of time. Recovery from NM damage with (*dashed*) and without (*solid*) TTHX1114 was evaluated by a histopathological grading scale (see Table 1 and Fig. 2). Values from the three categories were summed for each cornea to give the final grade. The dosing and administration of both NM and TTHX1114 were as described in Figure 3a.

3b. There was no significant difference between those exposed to TTHX1114 and those that were not. All images were graded with a score of 3 (data not shown). Interestingly, there was no evidence from these images of any hyperproliferative activity.

EdU Incorporation

To determine the extent to which TTHX1114 affords its protective effect against NM-induced cell damage/loss as manifested in the day 4 through day 9 period (Figs. 3a, 4) by stimulating the formation of new epithelial cells via proliferative stimuli, corneas exposed to NM and then treated with and without TTHX1114, as described in Figure 3, were treated with EdU (at 24 hours prior to the indicated time) and the labeled tissue analyzed by fluorescence microscopy (Fig. 5a, top row). The images were collected from the regions around the central lesion that were still populated with viable cells capable of proliferative responses. Clearly, corneas not exposed to TTHX1114 showed an increasing number of EdU-labeled cells from day 2 to 14 (Fig. 5b), with the percentage of cells incorporating EdU increasing from 19% to 68% ($P = 0.016$, Student's t-test), presumably reflecting the proliferation of epithelial cells that accompanies the normal regenerative process. The presence of TTHX1114 provides a rather different picture (Fig. 5a, bottom row). There is a much greater percentage of EdU-labeled cells at day 2, and this number diminishes over the next 12 days (Fig. 5b), reaching about the same level of incorporation as the untreated cells at day 2. Pairwise comparisons of NM versus NM+TTHX groups using the Student's t-test produce 2-tailed P values of 0.086, 0.40, 0.138, 0.069, and 0.083 at days 2 ,4, 6, 8, and 14, respectively. Thus, there is a trend toward a greater EdU incorporation in the cells that have already been exposed to TTHX1114 at short time periods after NM exposure, and this pattern inverts at day 14, with the TTHX1114-treated corneas having lower EdU incorporation and the NM-only corneas having greater EdU incorporation.

Effect of TTHX1114 on ADAM17 Expression Following NM Treatment

As NM attacks the epithelial cell layer, it induces microbullae at the epithelial-stromal junction, which is partially caused by cleavage of collagen XVII by ADAM17, and inhibition of this metalloprotease has been shown to be effective in preventing epithelial-stromal separation.[24] To assess whether TTHX1114 exerted any of its protective/proliferative response on NM-treated corneas, ADAM17 was imaged by immunofluorescence over 6 days following the NM lesion at both the site of the lesion (central) and in the periphery (Fig. 6). In naive cornea, ADAM-17 expression was seen localized to the area of the epithelial cells facing the basement membrane. As shown in the top row, at days 1, 4, and 6 following NM exposure, there was only a modest expression of ADAM17 in the periphery, and it was unchanged in this time frame. Little or no ADAM17 was detected in the lesion area during this period, consistent with a lack of epithelial cells in the center at these time points. When TTHX1114 was added (bottom row), there was a pronounced increase (compared to NM exposed) of ADAM17 at day 1 in both the lesion and peripheral areas. However, at the later time points, the effect of TTHX1114 on ADAM17 expression in the lesion site in treated corneas was basically identical to the untreated tissues, with little ADAM-17 expressed in the epithelial cells in the lesion area. ADAM17 levels in the peripheral cells remained similar to the naive cornea. Thus, TTHX1114, in contrast to expectations, did not lower ADAM17 and in fact increased its expression in cells removed from the lesion site. In all cases, ADAM-17 expression was localized in the epithelial cells to (1) the basement membrane facing area of the basal layer and (2) perinuclear cytoplasmic vesicles.

Effect of TTHX1114 on Stromal Keratocytes

As is well appreciated,[27] NM penetrates the stroma (and beyond), resulting in the loss of the keratocytes that populate this part of the cornea (see Fig. 3a). Stromal tissue from in vitro rabbit corneas, fixed and stained as described above, was evaluated for morphologic changes (Table 2). Changes in keratocyte morphology and loss were noted associated with the lesion site beginning with day 2. However, over all time points (days 2–14), no further changes in stromal organization, edema, or integrity was noted, either below or adjacent to the NM lesion sites (Fig. 7). TTHX1114 had no effect on these cells over this time frame. Keratocytes are known to be responsive to FGF-1, so the lack of response observed here may indicate that TTHX1114 does not readily penetrate the stroma to reach any reservoir of keratocytes that could serve as a source for new cells.

Expression of Native FGF-1 Following NM Treatment

To confirm that NM exposure impacts the levels of native FGF-1 in corneal epithelia, exposed corneas were analyzed by immunofluorescence at 1 and 3 days following NM treatment (Fig. 8). As compared to the controls, the NM-treated tissue showed no detectable FGF-1 in the epithelium after 1 day, although there were clearly detectable cells present. However, by day 3, a significant amount of FGF-1 was observed, indicating that FGF-1 expression is part of the normal regenerative process and that this process had already begun by this time point (in agreement with the EdU data shown in Fig. 5).
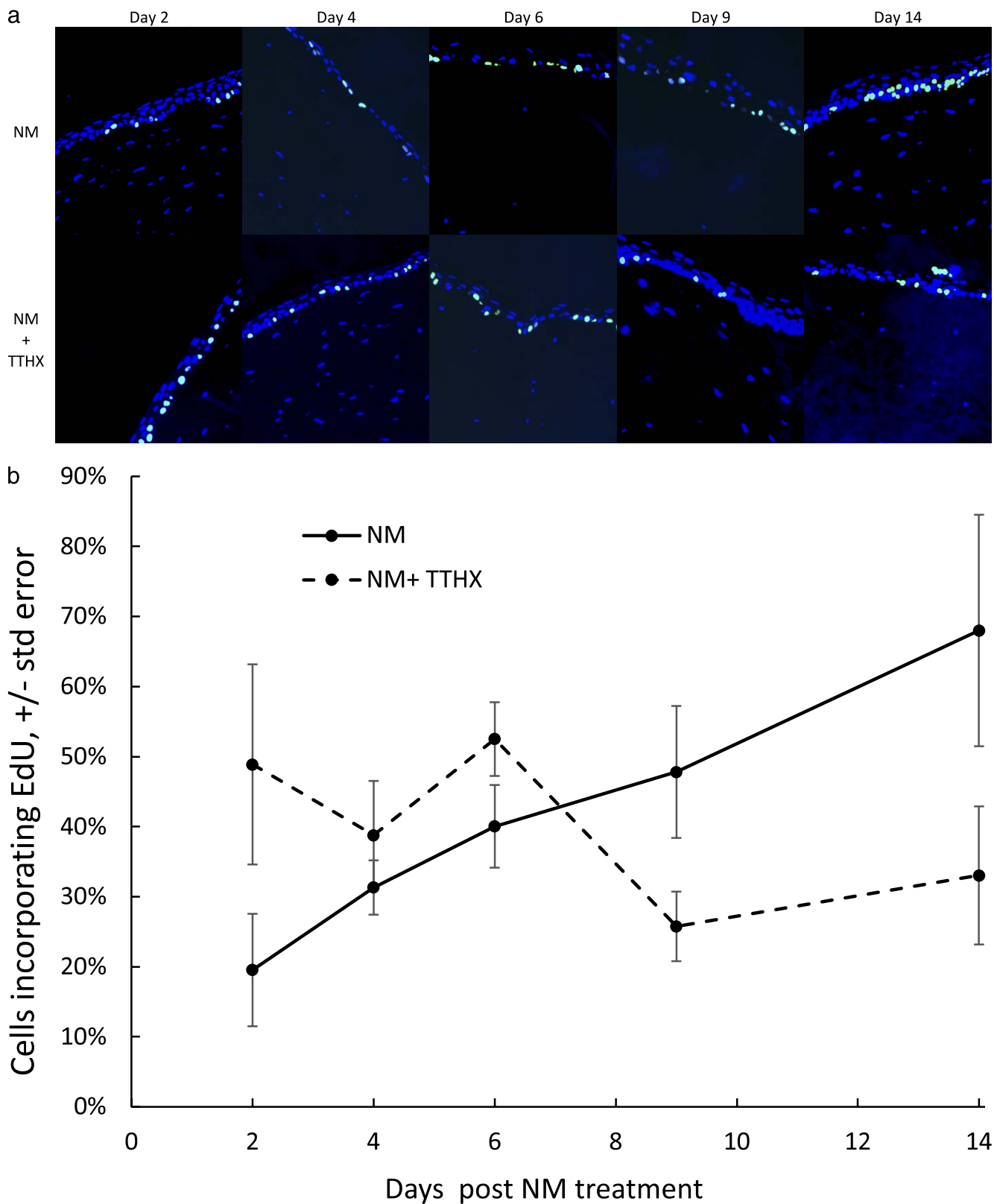
FIGURE 5. (a) Effect of TTHX1114 on corneal epithelial cells following NM damage as measured by EdU incorporation. Corneas in organ culture were treated with NM as described followed by incubation in media with (*bottom row*) or without (*top row*) TTHX1114 (100 pg/mL). Twenty-four hours prior to the times indicated, EdU-containing (10 pg/mL) media was added. Corneas were harvested at the indicated times post NM lesioning, fixed and stained for EdU with counterstain for Hoechst as described, and analyzed for EdU incorporation using fluorescence microscopy. Images were taken and analyzed from the peripheral cornea between the limbus and the edge of the NM lesion. (b) Percent of EdU incorporation in corneal epithelial tissue with (*dashed*) and without (*solid*) TTHX1114 treatment as a function of time. In vitro rabbit corneal epithelia peripheral to the NM lesion was counted for total number of EdU-labeled cells (numerator) divided by total number of basal cells (denominator).
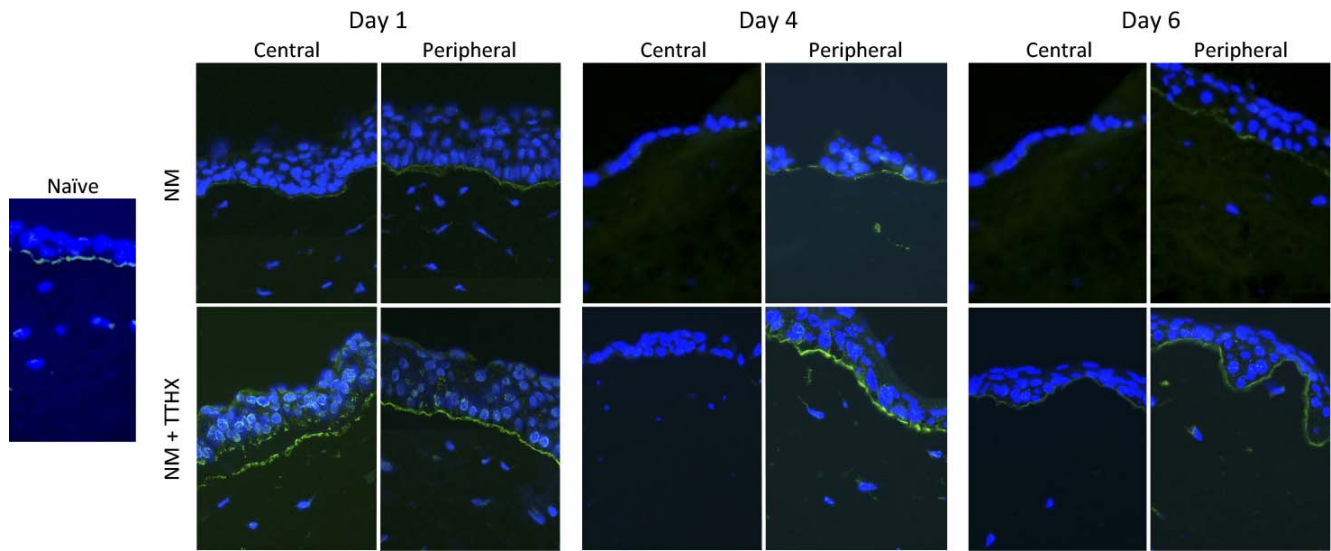
FIGURE 6. Induction of ADAM-17 by TTHX1114 treatment following NM exposure in rabbit corneal organ cultures. Corneas were cultured in vitro as described and treated with NM, rinsed, and cultured in media only (Control) or media supplemented with TTHX1114 (100 pg/mL). The naive section is a central corneal image from a cornea maintained in culture for 2 days but not treated with NM or TTHX1114. At the indicated times, corneas were embedded in OCT, frozen using a dry ice/isopentane solution, sectioned and stained with anti-ADAM17 antibody (*green*), and counterstained with DAPI (*blue*). Images were taken from the central cornea and from the peripheral cornea away from the area of NM damage. Sections were stained with anti-ADAM-17 (*green*) and DAPI (*blue*).

DISCUSSION

Cell viability is maintained in vivo by a complex network of factors and cell-cell interactions, which provide a combination of hypertrophic and hyperplastic stimuli that support it.[28] A significant portion of these activities are provided by humoral substances such as tissue growth factors and other endocrine-like modulators that arise locally (autocrine and/or paracrine) or systemically.[20] As a rule, these agents, such as epidermal growth factor, platelet-derived growth factor, and the transforming growth factor β family, are disulfide bond–containing entities. However, FGF-1 and -2, important members of this
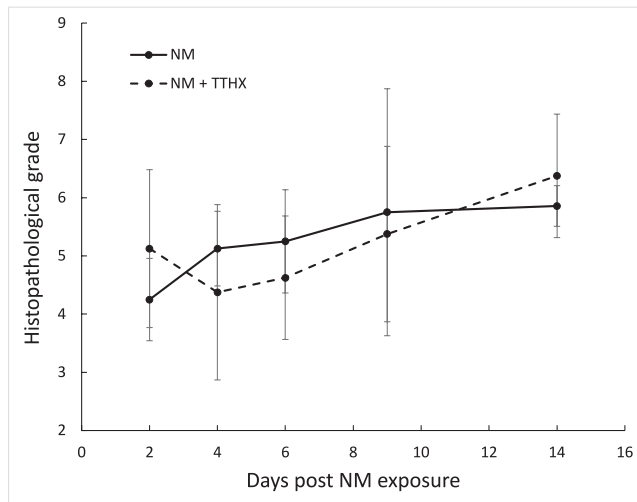

FIGURE 7. Effect of TTHX1114 on stromal keratocytes as a function of time following NM lesioning. Recovery from NM damage with (*dashed*) and without (*solid*) TTHX1114 was evaluated by a histopathological grading scale (see Table 2). Values from the two categories were summed for each cornea to give the final grade. The dosing and administration of both NM and TTHX1114 were as described in Figure 3a.
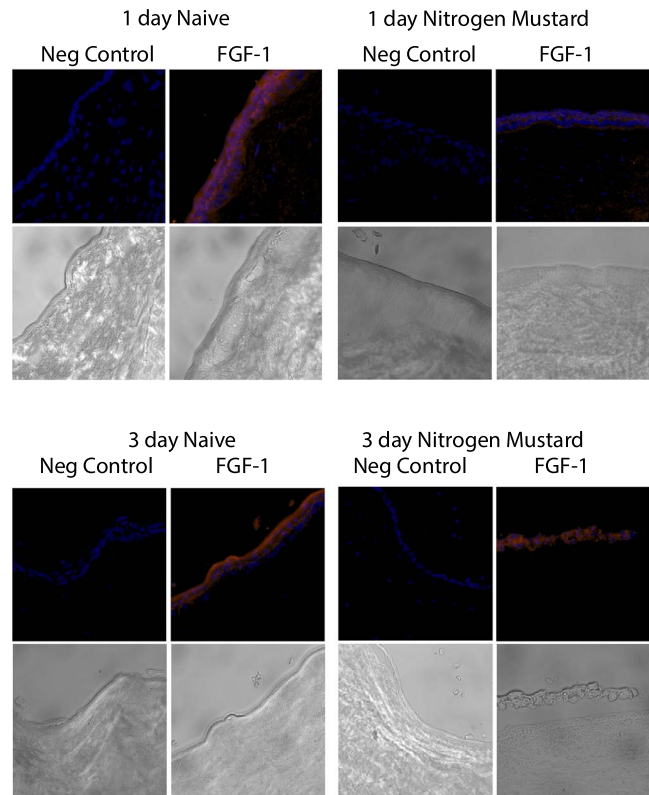
FIGURE 8. NM exposure reduces native FGF-1 levels in corneas cultured in vitro. Corneas were cultured and exposed to NM as described. Naive corneas or corneas 1 or 3 days after NM exposure were embedded in OCT, frozen, and 8- to 10-μm cryosections made and mounted on slides. Naive corneas were cultured in vitro for times matching the NM-exposed corneas. Slides were stained with (FGF-1) or without (negative control) anti-FGF-1 (Abcam 2E12) followed by donkey anti-mouse IgG (DyLight 549) as secondary antibody (*red*) and counterstained with DAPI (*blue*).

type of regulator, are exceptions in that they do not contain disulfide bonds and the three cysteines that are present are sensitive to modification that leads to inactivation.[21] As a result, native FGF-1(or -2) would be expected to be readily modified by NM,[10] and the vesicant would eliminate this source of trophic support for some window of time following exposure. Corneal epithelial cells are known to undergo proliferation in response to several growth factors,[19,20,29–31] including FGF-1,[14] and some of these have been exploited in wound-healing studies.[20] However, none have been shown to be particularly useful in accelerating the natural regenerative response following mustard gas exposure that generally takes a few weeks (but is dependent on the amount of vesicant used and the length of the exposure). These experiments demonstrate that an FGF-1 analog lacking cysteine residues has potent protective and regenerative effects following NM exposure. The pronounced response observed in these studies suggests that FGF-1 is a major component of that response and that natural healing, in the absence of added drug, is delayed until new FGF-1 can be synthesized (Fig. 6).

The characterization of vesicant damage of corneal tissues and the assessment of potential therapeutics to treat both acute and chronic manifestations of such exposure is constrained by the models available and the limitations on the use of the causative agents themselves. In this regard, NM, although not as potent as SM, can be handled safely with only modest special requirements as long as there is rigorous attention to good laboratory safety practices. Similarly, rabbit corneal organ cultures provide suitable test tissue that can be maintained in the laboratory for at least 2 weeks, which covers a significant part of the response to acute phase NM injury. In these studies, a rocker platform was modified to allow the cycling of fluid exposure of the tissue over a period of 2 hours such that it mimicked the natural lubrication of eyelid blinking and kept the corneas moist (Fig. 1). This arrangement also allowed the tissues to be constantly bathed in media containing the test drug sample.

When the corneal epithelium is first exposed to vesicant, there is a delay of several hours before symptoms are detected by the victim of the attack.[1] During that time, the agent is clearly causing damage to the cells of the corneal surface, and to the extent that it penetrates the stroma, on the keratocytes located there as well. Increasing evidence indicates that it can also reach the endothelial layer on the posterior surface and inflict damage on these cells. Indeed, the development of the chronic problems of mustard gas injury, or MGK, seems to be at least in part dependent on the extent of damage incurred by the endothelial cell layer during the acute phase of the insult.[32,33] There is certainly epithelial cell loss that occurs during this period (up to 2 days) that results from the modification of proteins/nucleic acids essential for viability.

These data do not specifically address the mechanisms by which TTHX1114 reduces NM damage and then aids in restoring epithelial function, but they suggest that two activities are likely involved. The reduction (improvement) in histopathological score and the observation that the epithelial layer is never completely eliminated suggests a reduction in the overall cytotoxicity of the NM and a potential anticytotoxic effect. On the other hand, the healing of the lesion requires the production of new epithelial cells, undoubtedly preceded by the migration of uninjured cells, from the periphery. The EdU data support this increased proliferation of the epithelial cells, and the lack of ADAM-17 in the epithelial cells that are protected or regenerating in the center of the lesion also indicates that cell adhesion to the stroma may be enhanced, favoring a role for cellular migration as well.

The protective/anticytotoxic actions of trophic factors have been observed in other paradigms involving cell damage and

death. For example, FGF is known to protect against radiation damage that can otherwise lead to cell death.[34,35] These effects are generally attributed to distinct changes in metabolism and other cell functions, and determining which of these may apply to protection against vesicant damage would be informative as a follow-up study. In the experiments described herein, topical application of vesicant to the cornea would be expected to most severely affect the cells closest to the ocular surface but be less damaging, that is, produce fewer modifications, in cells that are closer to the posterior side as the concentration of the vesicant decreased by diffusion. These more modestly impaired cells are much more likely to be rescuable through trophic support. In the absence of this support (because their source of trophic stimulation, i.e., native FGFs, has been inactivated by the vesicant), these same cells (or a significant percentage of them) would not survive, as observed in the control samples of Figure 4. Indeed, in the absence of any external trophic support, the epithelial cell losses usually extend across the entire lesion site, and the formation of new epithelial cells must occur in the areas surrounding the lesion or in the periphery (limbus). While from these data it is not possible to determine the relative contributions of new epithelial cell formation, stimulated by TTHX1114 and a protective effect afforded by providing trophic support to replace that normally provided by native FGF-1, it seems likely that both mechanisms underlie the overall amelioration observed.

NM is an alkylating agent that has been shown to modify Lys and His side chains as well as those of Cys. Adduction likely occurs via the initial formation of a reactive aziridinium, intermediately followed by covalent reaction.[10] All nucleophiles in proteins are pH sensitive (except the thioether of methionine), and lysine is poorly reactive at neutrality, but the other two would likely be modified under the conditions of these experiments. Cys is about an order of magnitude more reactive than His. Thus, any proteins containing Cys, where their modification impacts activity, will be particularly susceptible to mustard gas. It may be imagined that the cytoplasm of mammalian cells is rich in proteins that generally meet this description, and thus it may be further concluded that once NM has penetrated the plasma membrane, cellular damage that is largely irreversible will occur. It would be of substantial interest to understand how TTHX1114 can offset such damage via trophic stimulation.

The application of NM to the organ cultures is necessarily difficult to quantify. In the experiments reported herein, NM was added topically as a drop of reagent solution in a fixed volume. Over the course of several experiments, some variation was observed in the severity of the lesion introduced (e.g., Fig. 3b, day 6), but the time of response, with and without TTHX1114 treatment, was not altered. When NM was delivered by soaking a 6-mm circle of filter paper with reagent and placing it on the anterior surface of the cornea, it was determined that the NM lesion extended to the limbus, although it did not appear to penetrate the stroma to the same extent. Thus, this method of application tended to diffuse the vesicant laterally over a larger surface area with less penetration (data not shown). This method was not used in the studies reported herein. These differences related to drug application also underscore the difficulty in comparing responses to damage introduced by different vesicants, for example, NM and SM.

The observations in this report support the view that TTHX1114 exerts a positive effect on NM-induced lesions of the corneal epithelium. In other experiments, TTHX1114 has also been shown to induce a similar response in vivo to lesions introduced by SM in rabbits (unpublished observations). Although the onset of the cell losses was faster than in the organ culture experiments, the overall impact of TTHX1114 on

the healing process as measured by pachymetry and corneal fluorescein staining was similar to those reported here. These experiments were conducted with a twice daily topical dosing regimen of TTHX1114. Taken together with the organ culture results described in this report, it suggests that TTHX1114 is a potentially useful drug for addressing vesicant damage to the corneal epithelium that could be delivered in an eyedrop fashion.

References

1. Papirmeister B, Feister AJ, Robinson SI, Ford RD. *Medical Defense Against Mustard Gas: Toxic Mechanisms and Pharmacological Implications*. Boca Raton, Florida: CRC Press; 1991:21–23,61–66.

2. Javadi MA, Yazdani S, Kanavi MR, et al. Long-term outcomes of penetrating keratoplasty in chronic and delayed mustard gas keratitis. *Cornea*. 2007;26:1074–1078.

3. McNutt P, Hamilton T, Nelson M, et al. Pathogenesis of acute and delayed corneal lesions after ocular exposure to sulfur mustard vapor. *Cornea*. 2012;31:280–290.

4. Tewari-Singh N, Jain AK, Inturi S, et al. Silibinin, dexamethasone, and doxycycline as potential therapeutic agents for treating vesicant-inflicted ocular injuries. *Toxicol Appl Pharmacol*. 2012;264:23–31.

5. Baradaran-Rafii A, Eslani M, Tseng SC. Sulfur mustard-induced ocular surface disorders. *Ocul Surf*. 2011;9:163–178.

6. Goswami DG, Tewari-Singh N, Agarwal R. Corneal toxicity induced by vesicating agents and effective treatment options. *Ann N Y Acad Sci*. 2016;1374:193–201.

7. Baradaran-Rafii A, Javadi MA, Karimian F, Feizi S. Mustard gas induced ocular surface disorders. *J Ophthalmic Vis Res*. 2013;8:383–390.

8. Feizi S, Javadi MA, Jafarinasab MR, Karimian F. Penetrating keratoplasty versus lamellar keratoplasty for mustard gas-induced keratitis. *Cornea*. 2013;32:396–400.

9. Goswami DG, Tewari-Singh N, Dhar D, et al. Nitrogen mustard-induced corneal injury involves DNA damage and pathways related to inflammation, epithelial-stromal separation and neovascularization. *Cornea*. 2016;35:257–266.

10. Thompson VR, DeCaprio AP. Covalent adduction of nitrogen mustards to model protein nucleophiles. *Chem Res Toxicol*. 2013;26:1263–1271.

11. Braakman I, Bulleid NJ. Protein folding and modification in the mammalian endoplasmic reticulum. *Annu Rev Biochem*. 2011;80:71–99.

12. Nickel W, Steringer JP, Mueller H-M, Brough D. Unconventional protein secretion: fibroblast growth factor 2 and interleukin-1β as examples. In: Bradshaw RA, Stahl PD, eds. *Encyclopedia of Cell Biology*. Oxford: Academic Press: 2016; II:520–527.

13. Ornitz DM, Itoh N. The fibroblast growth factor signaling pathway. *Wiley Interdiscip Rev Dev Biol*. 2015;4:215–266.

14. Dabin I, Courtois Y. Acidic fibroblast growth factor overexpression in corneal epithelial wound healing. *Growth Factors*. 1991;5:129–139.

15. Zhang J, Upadhya D, Lu L, Reneker LW. Fibroblast growth factor receptor 2 (FGFR2) is required for corneal epithelial cell proliferation and differentiation during embryonic development. *PLoS One*. 2015;10:e0117089.

16. Wilson SE, He Y-G, Lloyd SA. EGF, basic FGF, and TGFβ messenger RNA production in rabbit corneal epithelial cells. *Invest Ophthalmol Vis Sci*. 1992;33:1987–1995.

17. Wilson SE, Lloyd SA, He Y-G. Fibroblast growth factor-1 receptor messenger RNA expression in corneal cells. *Cornea*. 1993;12:249–254.

18. Wilson SE, Walker JW, Chwang EL, He Y-G. Hepatocyte growth factor, keratinocyte growth factor, their receptors, fibroblast growth factor receptor-2, and the cells of the cornea. *Invest Ophthalmol Vis Sci*. 1993;34:2544–2561.

19. Meduri A, Aragona P, Grenga PL, Roszkowska AM. Effect of basic fibroblast growth factor on corneal epithelial healing after photorefractive keratectomy. *J Refract Surg*. 2012;28:220–223.

20. Baldwin HC, Marshall J. Growth factors in corneal wound healing following refractive surgery: a review. *Acta Ophthalmol Scand*. 2002;80:238–247.

21. Ortega S, Schaeffer M-T, Soderman D, et al. Conversion of cysteine to serine residues alters the activity, stability, and heparin dependence of acidic fibroblast growth factor. *J Biol Chem*. 1991;266:5842–5846.

22. Culajay JF, Blaber SI, Khurana A, Blaber M. Thermodynamic characterization of mutants of human fibroblast growth factor 1 with an increased physiological half-life. *Biochemistry*. 2000;39:7153–7158.

23. Xia X, Kumru OS, Blaber SI, et al. Engineering a cysteine-free form of human fibroblast growth factor-1 for "second generation" therapeutic application. *J Pharm Sci*. 2016;105:1444–1453.

24. DeSantis-Rodrigues A, Chang YC, Hahn RA, et al. ADAM17 inhibitors attenuate corneal epithelial detachment induced by mustard exposure. *Invest Ophthalmol Vis Sci*. 2016;57:1687–1698.

25. Gordon MK, DeSantis A, Deshmukh M, et al. Doxycycline hydrogels as a potential therapy for ocular vesicant injury. *J Ocul Pharmacol Ther*. 2010;26:407–441.

26. Fischer AH, Jacobson KA, Rose J, Zeller R. Hematoxylin and eosin staining of tissue and cell sections. *Cold Spring Harb Protoc*. 2008;2008:pdb.prot4986.

27. McNutt P, Lyman M, Swartz A, et al. Architectural and biochemical expressions of mustard gas keratopathy: preclinical indicators and pathogenic mechanisms. *PLoS One*. 2012;7:e42837.

28. Goss RJ. Hypertrophy versus hyperplasia. *Science*. 1966;153:1615–1620.

29. Wang L, Wu X, Shi T, Lu L. Epidermal growth factor (EGF)-induced corneal epithelial wound healing through nuclear factor kB subtype-regulated CCCTC binding factor (CTCF) activation. *J Biol Chem*. 2013;288:24363–24371.

30. Huang Y-H, Ching-Chang I, Kuo C-H, et al. Thrombomodulin promotes corneal epithelial wound healing. *PLoS One*. 2015;10:e0122491.

31. Zhou Q, Chen P, Di G, et al. Ciliary neurotrophic factor promotes the activation of corneal epithelial stem/ progenitor cells and accelerates corneal epithelial wound healing. *Stem Cells*. 2015;33:1566–1576.

32. McNutt PM, Tuznik KM, Glotfelty EJ, et al. Contributions of tissue-specific pathologies to corneal injuries following exposure to SM vapor. *Ann NY Acad Sci*. 2016;1374:132–143.

33. McNutt P, Tuznik K, Nelson M, et al. Structural, morphological, and functional correlates of corneal endothelial toxicity

following corneal exposure to sulfur mustard vapor. *Invest Ophthalmol Vis Sci*. 2013;54:6735–6744.

34. Li YQ, Chen P, Haimovitz-Friedman A, Reilly RM, Wong CS. Endothelial apoptosis initiates acute blood–brain barrier disruption after ionizing radiation. *Cancer Res*. 2003;63: 5950–5956.

35. Wong CS, Fehlings MG, Sahgal A. Pathobiology of radiation myelopathy and strategies to mitigate injury. *Spinal Cord*. 2015;53:574–580.